A COMPARISON OF TRAJECTORY GENERATION ALGORITHMS FOR A TERRAIN FOLLOWING FLIGHT

Hyunju Lee[1], Sangchul Lee[1]

[1]Department of Smart Air Mobility, Korea Aerospace University, Goyang 10540, Korea

Abstract

Terrain following (TF) flight leads to low altitude fly while preventing the collision with the ground. For safe and effective TF flight, an appropriate trajectory must be generated. Typically, the terrain information for TF flight can be obtained from a digital terrain database and radar. There are several methods available for generating the trajectory. This paper compares two TF trajectory generation methods that use radar scan data for terrain information. The comparison is conducted through the simulations with several scenarios. The simulation results are analyzed, revealing that the outcomes of both methods are similar. Based on the simulation results, improvements to the existing TF trajectory generation methods are proposed.

Keywords: Terrain Following, Trajectory, 3-mask morphology, NPR algorithm

1. Introduction

In military aviation, TF plays a crucial role, offering the capability for aircraft to fly close to the ground to minimize the risk of detection by enemies. Maintaining a flightworthy trajectory, with a specific clearance height over terrain, is essential to avoid collisions with the ground. Accurate acquisition of terrain information is necessary to provide a precise trajectory, which can be obtained from a radar and a digital terrain database [1,2,3]. The terrain profile can be generated using radar scan data, a digital terrain database, or a combination of both. However, radar scan data may have limitations due to the radar's maximum range. Generally, TF predominantly considers longitudinal motion along the aircraft's path, allowing for the generation of a 2-dimensional terrain profile [2, 3]. This terrain profile serves as the foundation for the TF trajectory.

Researchers have addressed TF trajectory generation problems by applying concepts of optimal control and optimization [4, 5]. A cubic-B-Spline is utilized to approximate the optimal TF trajectory and determine the coefficients of the spline to minimize altitude error, thus generating the optimal trajectory [5]. The inverse dynamics approach has been applied to deal with the optimal TF trajectory and generating TF trajectory using sequential quadratic programming [6]. The objective of the research is to minimize the flight time and the altitude difference with terrain. However, generating a TF trajectory using the optimal control or optimization can be challenging to apply in real time due to the computational complexity, and it often requires a significant time to derive results or failing to converge to a solution [7]. Besides optimal control and optimization, several methods for generating TF trajectories exist, including geometric concept and reshaping concept. The trajectory reshaping algorithm generates the TF trajectory by using the nearby terrain information and reshaping the trajectory according to the constraints [8].

In this paper, two methods are analyzed within a two-dimensional space under several flight scenarios. One method is the 3-mask morphology and circular path method [9] which incorporates geometric concepts, while the other uses neighbor point re-positioning (NPR) which employs reshaping concepts [10]. Comparing these methods can provide insights into potential improvements. Brief introductions of the two algorithms are provided in Chapter 2. Chapter 3 analyzes the two methods in two-dimensional space under several flight scenarios. Future work and conclusions are presented subsequently.

2. TF trajectory generation methods

TF trajectory generation methods, using 3-mask morphology and circular path method, and using NPR algorithms, assumed that the terrain profile is generated using radar scan data gathered in a DTED (Digital Terrain Elevation Database) Level 2 environment. The terrain profile depicted in Fig. 1 serves as an example of terrain information for TF. This terrain profile maintains a similar altitude with the terrain up to 4km away from the aircraft's position. TF trajectory is generated based on the two-dimensional terrain profile over this 4km distance [11].

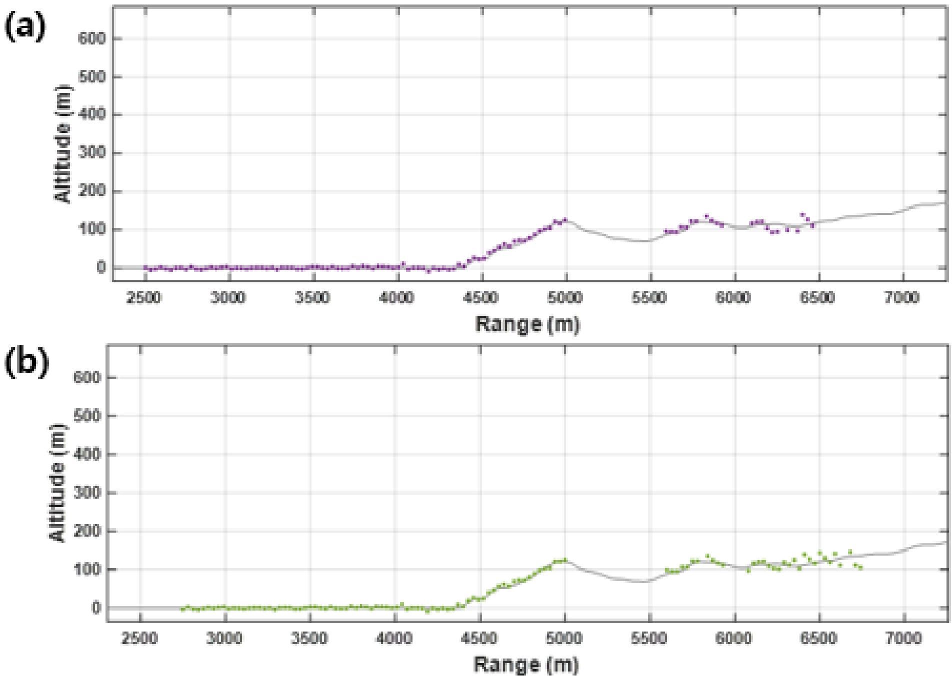

Figure 1 – Terrain profile.

2.1 3-mask morphology and circular path method

The trajectory generation method using 3-mask morphology and circular path method involves two main steps: generating TF path and generating TF trajectory. 3-mask morphology is employed to generate the TF path without considering time, while the circular path method is utilized to generate the TF trajectory, which incorporates the time concept. Figure 2 provides an overview of 3-mask morphology and circular path method. In the first step, 3-mask morphology is used to generate the TF path, ensuring it satisfies the clearance height and clime/dive angle limits. Subsequently, the circular path method is employed to smooth the TF path, and it satisfies the normal acceleration limits and climb/dive angle limits. After generating the TF path using these methods, the path is converted into a TF trajectory. Assuming a constant aircraft speed, TF path consists of circular segments and straight segments. Then, this path is converted into a trajectory that specifies the position, speed, and flight path angle. During this conversion, the guidance command (G-cmd), representing the normal acceleration, is generated. After an internal tracking phase, the G-command is refined to ensure accurate trajectory following.

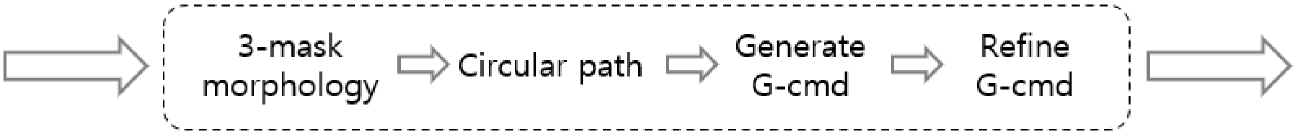

Figure 2 – Overview of 3-mask morphology and circular path method.

Figure 3 provides an example of TF trajectory based on 3-mask morphology and circular path. In this case, the active mode profile, which uses the radar scan data, serves as reference path. As described in [9], the tracking simulation was conducted using a very simple aircraft kinematic model, resulting in the calculation of the climb/dive angle and normal acceleration.

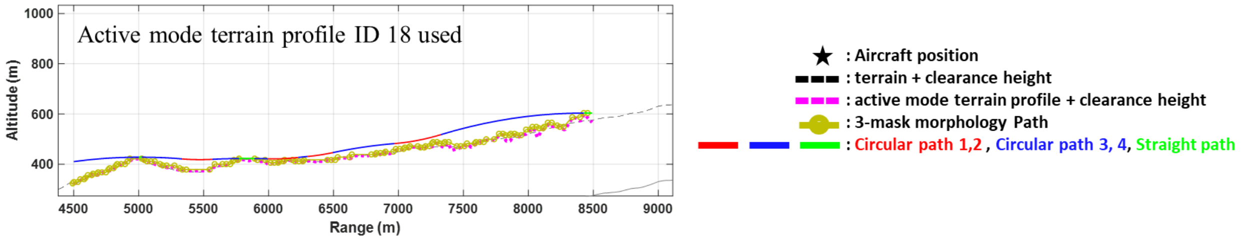

Figure 3 – Example of TF trajectory based on 3-mask morphology and circular path method.

2.2 NPR algorithm

The trajectory generation algorithm using NPR algorithm is also designed for constant aircraft speed. his algorithm utilizes constraints such as push-down/pull-up acceleration, climb/dive angle, and vertical acceleration while generating the trajectory. Figure 4 illustrates an example of a TF trajectory generated using NPR algorithm. The left figure depicts the generation trajectory, while the right figure shows the constrains, including vertical velocity, vertical acceleration, and jerk.

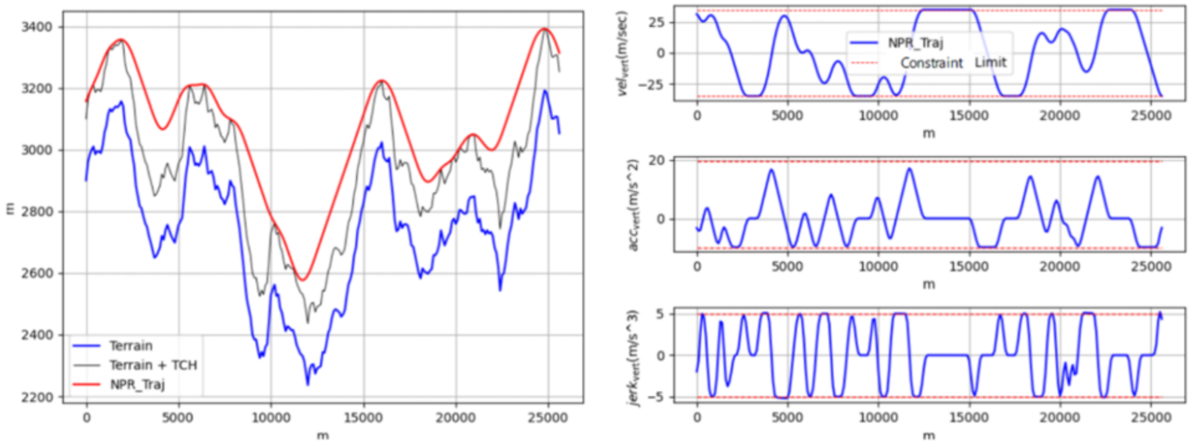

Figure 4 – Example of TF trajectory based on NPR algorithm.

3. Simulation

3.1 Simulation conditions

Since these two methods uses slightly different terrain profiles and inputs, the first step involves the aligning the input and output of both methods. The inputs are shown in Table 1 and the outputs consist of the generated trajectories and g-command. Due to the roughness of the terrain, moderate terrain and rough terrain are selected as shown in Fig. 5. Both methods are used to generate TF trajectories in these two cases. The simulations are conducted under several scenarios. Under the straight flight condition, both single cycle and multiple cycle simulation are performed. The single cycle represents the process of the trajectory generation with one cycle of active mode terrain profile, which includes only 4km of the terrain information. The multiple cycle uses 10 cycle of active mode terrain profiles, each cycle covering 4km. Each cycle is generated for every 2km of flight, resulting in a total of 20 km of TF trajectory.

Table 1 – Simulation conditions

Input	Setting
Aircraft speed	250 m/sec
Flight path angle limit	-15 ~ 30 deg
Normal acceleration limit	-0.9 ~ 2.0g
Initial flight path angle	0 deg
Initial pitch angle	0 deg
Terrain clearance height (TCH)	300 m

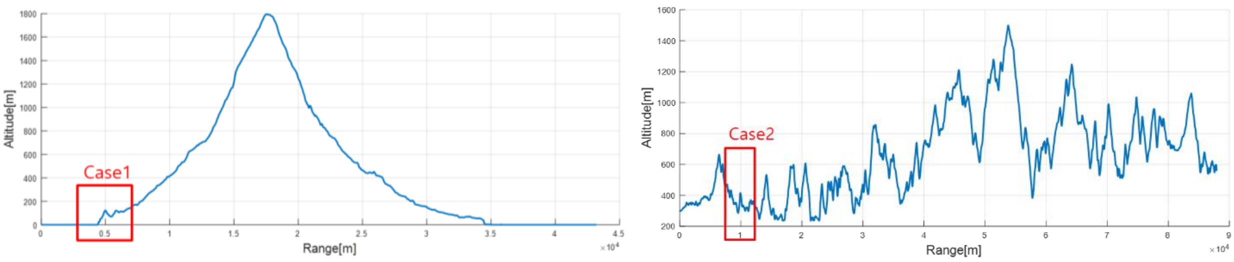

Figure 5 – Simulation cases.

3.2 Simulation results

Figure 6 shows the results for a single cycle. In these figures, the red line represents 3-mask morphology and circular path method, while the blue line represents the NPR algorithm. The left figure depicts the TF trajectory shown as red and blue line while the sky-blue line represents terrain profile, and the orange line indicates the combination of terrain profile and TCH. The constraints, such as the normal velocity and the g-command, are shown on the right side. The normal velocity is calculated as Eq. (1). The generated trajectories and the constraints are similar for both methods. 3-mask morphology and circular path method generated a slightly higher trajectory, whereas NPR algorithm generated trajectories closer to the combination of terrain profile and TCH. Both methods satisfy all the constraints' limitations. Specifically, the altitude error from TCH, satisfaction with FPA 0°, and the satisfaction of constraint conditions at the peak point of the generated trajectory are analyzed. At the peak point, when observing the FPA, 3-mask morphology and circular path method maintains values within an error range of ±5° and when observing the error from TCH, it maintains values within an error range of ±4m, while NPR algorithm consistently satisfies 0 in all cases.

$$Normal\ velocity = 250 \times \sin\gamma \quad (\gamma = climb/dive\ angle) \tag{1}$$

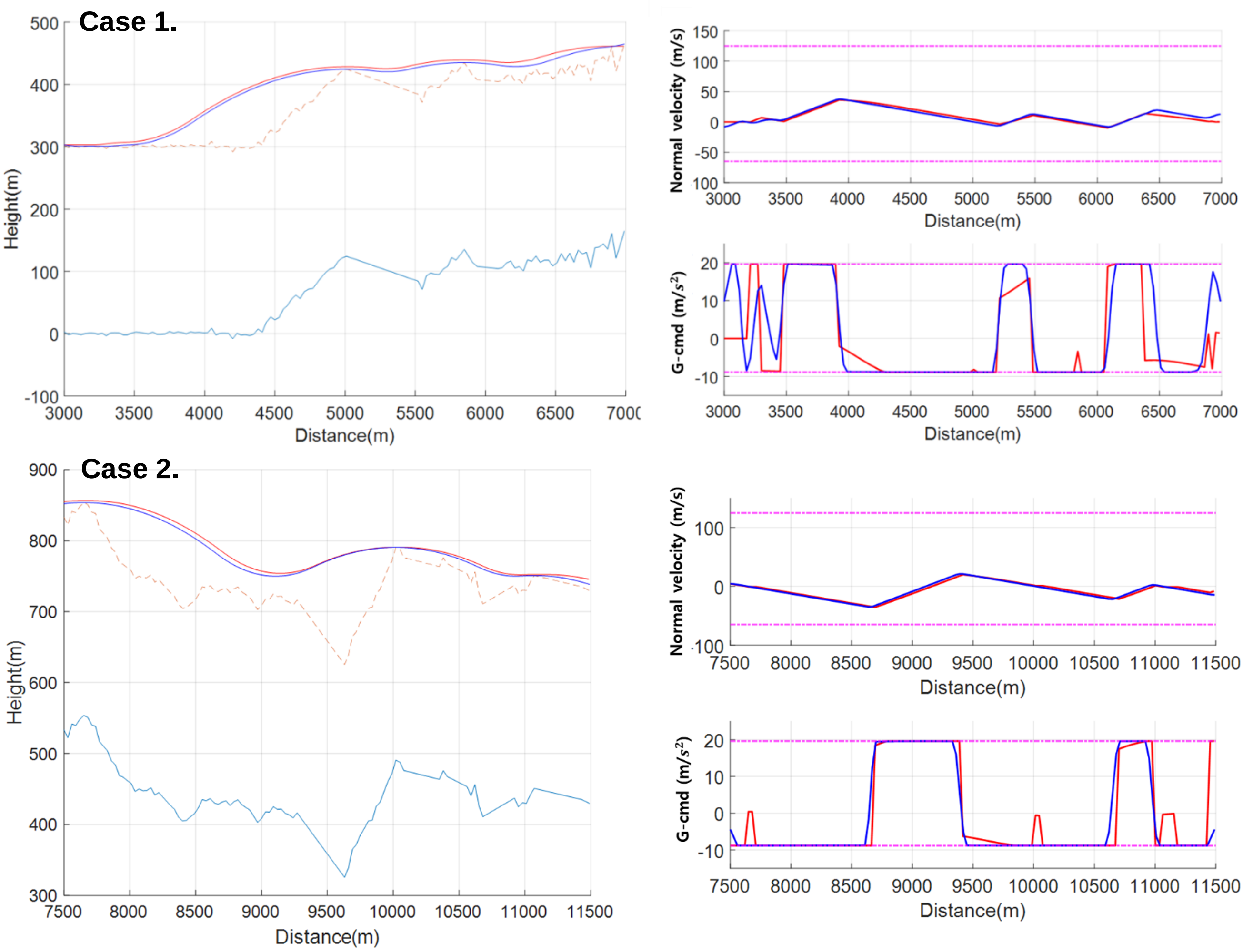

Figure 6 – Single cycle cases.

To figure out whether the generated trajectory is flightworthy or not, the tracking simulation was conducted. The tracking simulation uses a point mass model as Eq. (2) enabling it to follow the given g-command, which has rapid changes. The tracking model is illustrated in Fig. 7.

$$\dot{x} = V cos\gamma \text{ , } \dot{h} = V sin\gamma, \dot{V} = a_{t,rot} \text{ , } \dot{\gamma} = \frac{a_{n,rot}}{V} \tag{2}$$

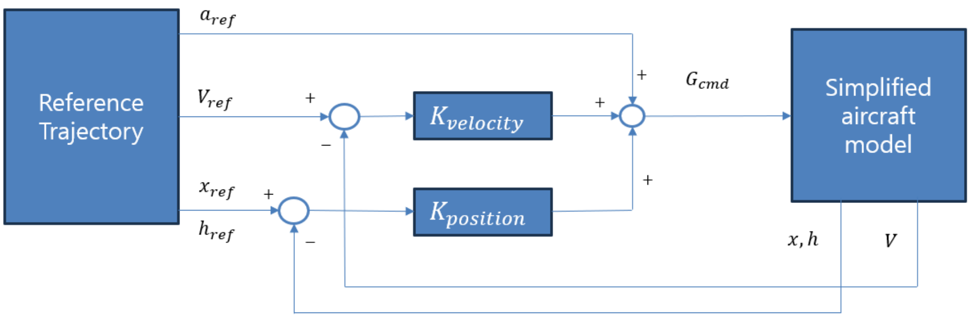

Figure 7 – Tracking model.

Figure 7 illustrates the tracking results of each single cycle. The reference trajectory, represented by the red line in Fig. 8, is the outcome of each algorithm and the green line depicts the tracking results. Owing to the g-command shown in Fig. 6, the 3-mask morphology and circular path method track the trajectory more effectively than the NPR algorithm. 3-mask morphology and circular path method include an internal tracking simulation phase to refine the g-command, resulting in a final output that is more suitable for flight compared to the NPR algorithm.

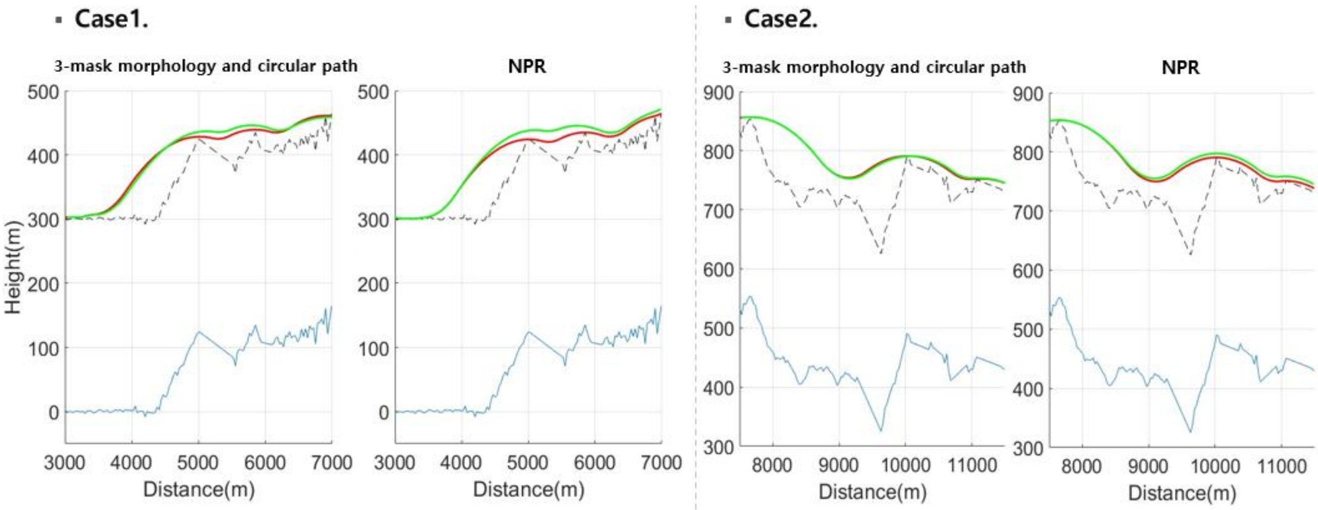

Figure 8 – Tracking results of single cycle cases.

Next, the multiple cycle cases are simulated. 3-mask morphology and circular path method generates the trajectory by considering both the current terrain profile and the previous cycle's trajectory, whereas NPR algorithm only considers the current terrain profile. Consequently, the reference trajectories from NPR algorithm are not continuous every 2km. Figure 9 presents the results of multiple cycle cases. The results of tracking 10 cycles of trajectories are shown on the left side, and the constraints are shown on the right side. The red and blue lines represent the reference trajectories every 2km, while the green line indicates the tracking result. The discontinuity in NPR algorithm's reference trajectories may impact tracking performance. Larger gaps between reference trajectories can make it more challenging to follow the intended path. In rough terrain, as illustrated in case 2, even the 3-mask morphology and circular path method can encounter difficulties in tracking, despite having connected reference trajectories.

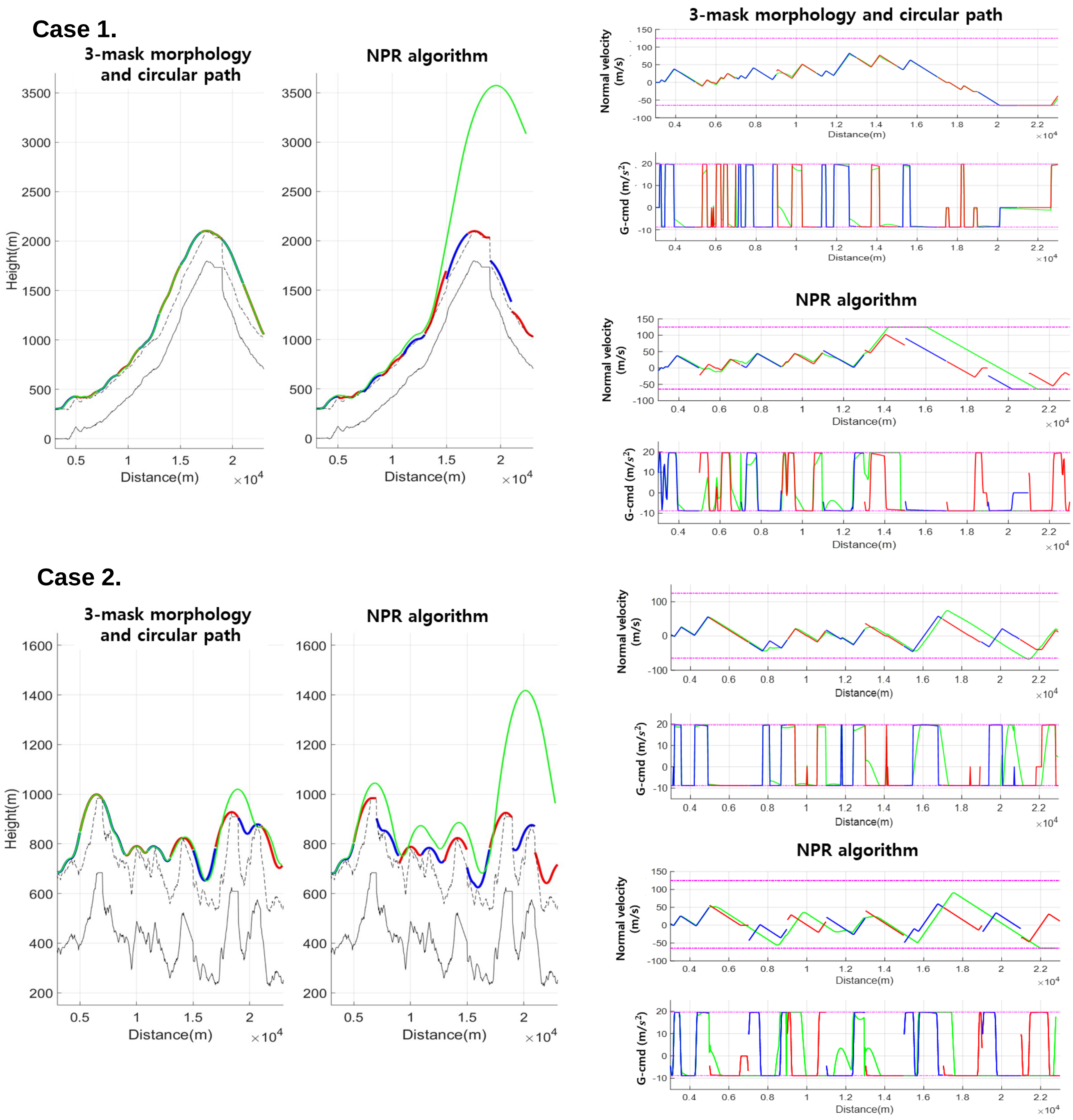

Figure 9 – Tracking results and constraints of multiple cycle cases.

3.3 Analysis of the results

Based on the simulation results, it is observed that for both case 1 and case 2, the flight trajectories generated by both methods for a single cycle are similar. Similar results are also obtained for climb/dive angles and g-command. At the peak point, where FPA (Flight Path Angle) 0° must be satisfied, NPR algorithm fulfills FPA 0° in all cases and maintains zero error with TCH at the peak point. However, 3-mask morphology and circular path method incurs slight errors in both aspects. During the process utilizing 3-mask morphology technique, the grids are formed as shown in Fig. 10. While this process can generate paths that satisfy the climb/dive angle limits for all terrain profiles, the grids may form at positions higher than the terrain profile. Therefore, due to the influence of these grids, discrepancies in altitude may occur between 'terrain profile + TCH' and the generated flight trajectory.

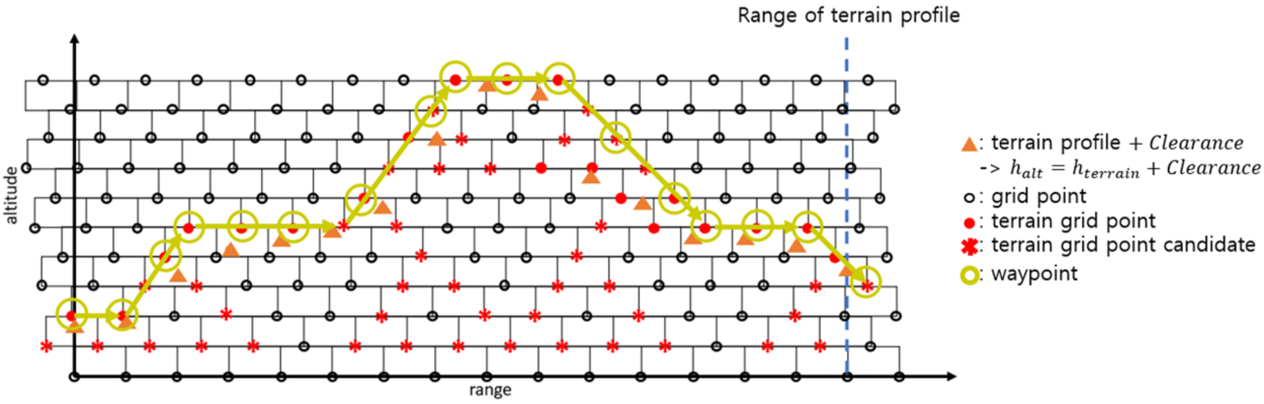

Figure 10 – 3-mask morphology method.

In the case of multiple cycles, it was observed that 3-mask morphology and circular path method tracks relatively similar trajectories to the reference trajectory. This phenomenon arises because this method automatically generates the trajectory by considering the previous trajectory at the point 2 km after the completion of the previous cycle within the method. However, for NPR algorithm, when generating multiple cycles, a new flight trajectory is created based on the terrain profile at the point where the trajectory is generated for each new cycle. As shown in Fig. 11, when generating two cycles, while 3-mask morphology and circular path method ensures that the trajectory at the beginning of the 2nd cycle matches that of the 2 km point in the preceding 1st cycle, NPR algorithm may introduce errors between the trajectory at the 2 km point in the preceding 1st cycle and the initial conditions of the 2nd cycle.

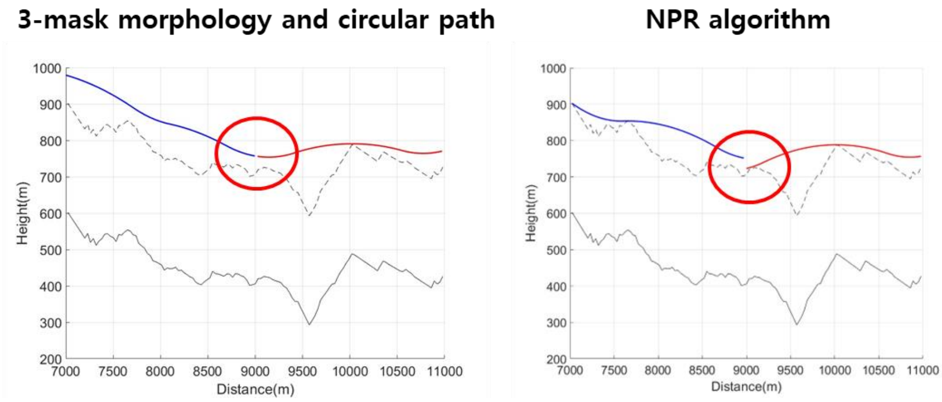

Figure 11 – Continuity of two cycles.

From the simulation results, certain limitations of each method have been identified. These insights can be valuable for improving existing TF trajectory generation methods. First, to implement 3-mask morphology and circular path method effectively, careful consideration of the grid formation illustrated in Fig. 12 is necessary. The size of the grid can be determined by the interval of the terrain profile and climb/dive angle limit. As the grid size decreases, the likelihood of staying close to the combination of terrain profile and TCH increases. Therefore, refining the grid size by adjusting the terrain profile's interval or climb/dive angle limit could be beneficial.

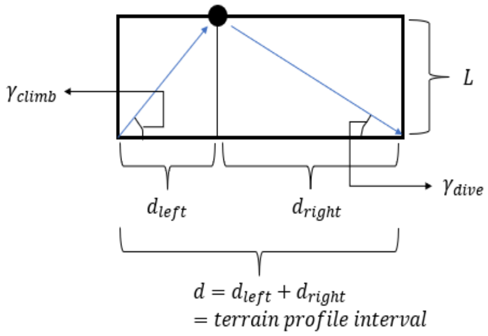

Figure 12 – Grid formation of 3-mask morphology.

Although reducing the grid size can improve the trajectory accuracy in many cases, there are instances where the FPA and error with TCH may not be zero at certain peak points. In such cases, an alternative approach, such as the brute force method [12], could be employed. As depicted in Fig. 13, the brute force is similar to trajectory reshaping. When the reference waypoint is a non-flyable path, waypoint candidate will be generated to satisfy the constraints. Unlike 3-mask morphology method, the brute force method does not require grid formation. Consequently, the reference waypoint can be positioned more closely to the combination of terrain profile and TCH. Following the brute force method, the circular path method can be utilized to further refine the trajectory into a flightworthy path.

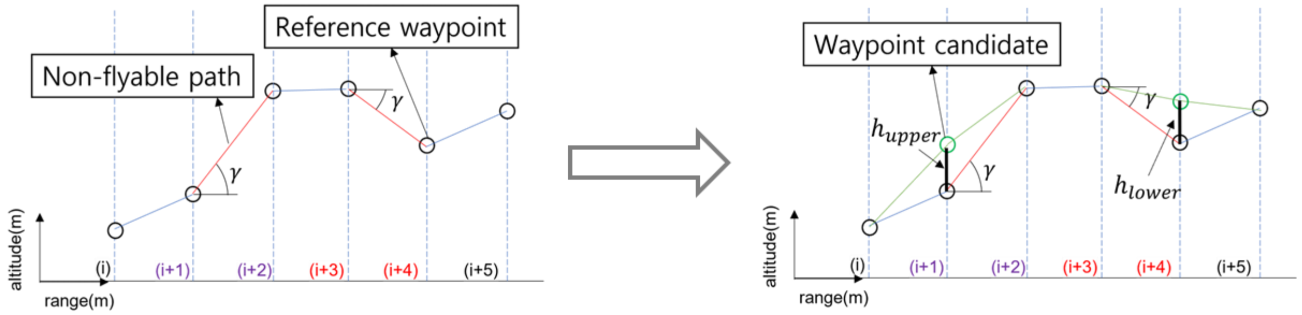

Figure 13 – Brute force method.

Figure 14 depicts a comparison between 3-mask morphology method and the brute force method. During the climbing and diving phases, the brute force method may result in a higher altitude compared to the 3-mask morphology method. However, at the peak point, the results are reversed. While the brute force method may generate a higher path during the climbing and diving phases, the application of the circular path method could offset this higher altitude.

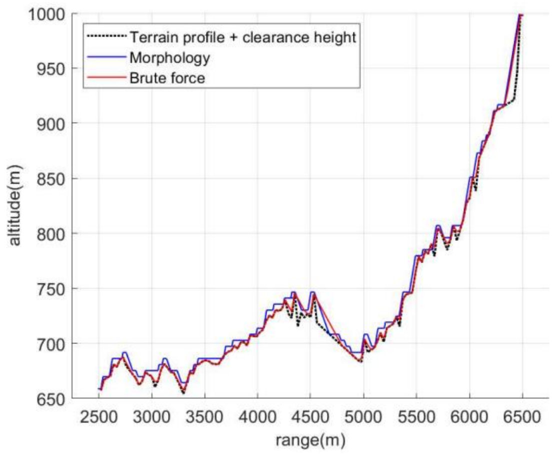

Figure 14 – Comparison of 3-mask morphology and brute force.

Indeed, the current output of existing methods, such as g-command, poses challenges for flight due to its rapid changes. Although the tracking simulation uses a point mass model, there are some bumping phenomena. Despite employing a point mass model in the tracking simulation, bumping phenomena still occur. This issue becomes particularly problematic during multiple cycles, especially in rough terrain. To address this problem, it may be effective to consider jerk in controlling the g-command. As depicted in Fig. 6, rapid changes in the g-command are evident. Aligning the jerk limitation or refining the logic of jerk generation could result in smoother changes in the g-command, thereby enhancing flightworthiness.

Moreover, the simulations are limited to straight flight cases due to the constraints of the two-dimensional terrain profile. It is imperative to conduct simulations for lateral directional flight cases as well. Among various approaches to address this challenge, updating the 3D terrain map and generating the terrain profile based on this updated terrain map could be a viable solution.

4. Conclusion

In this paper, trajectory generation algorithms for terrain following (TF) utilizing geometric and reshaping concepts are introduced. A comparison is made between a method employing 3-mask morphology and circular path and another method utilizing the NPR algorithm across various flight scenarios. In the single cycle analysis, 3-mask morphology and circular path method generated peak points where FPA maintained values within an error range of ±5° and the error from TCH remained within an error range of ±4m, while the NPR algorithm consistently satisfied FPA 0° in all cases. In multiple case scenarios, 3-mask morphology and circular path method exhibited more robust results than the NPR algorithm. Since both methods exhibit limitations during tracking simulation, the brute force method and incorporating jerk logic could be concerned to address the limitations. Jerk control can lead to the generation of more flightworthy g-command, potentially enhancing the aircraft's ability to effectively track the generated TF trajectory. Additionally, in order to handle the lateral directional cases, the development of a map updating process could be one of the solutions.

5. Contact Author Email Address

For further communication, the author’s email address is shown as follows.

Hyunju Lee: hyunju@kau.kr

6. Copyright Statement

References

[1] Fountain J R. Digital Terrain System. Workshop on Airborne Navigation Systems, doi: 10.1049/ic:19970909, 1997

[2] Oxley, P. C. Terrain Following and Terrain Avoidance Algorithms. IEE Colloquium on Navigation, Guidance and Control on Aerospace, pp. 1-2, 1989

[3] Starling R. J., & Stewart C M. The Development of Terrain Following Radar. Aircraft Engineering and Aerospace Technology, doi: 10.1108/eb034756, 1971

[4] Malake, S. M., & Kosari, A. R. (2007). Novel Minimum Time Trajectory Planning in Terrain Following Flights. IEEE Transactions on Aerospace and Electronic Systems, 43(1), 2-12.

[5] Kim, H. S., Lee, S. M. & Park, S. O. (1994). A Study on the Optimal Terrain Following using Cubio-B-Spline Function. Journal of the Korean Society for Aeronautical and Space Sciences, 22(4), 109-118.

[6] Lu, P., & Pierson, B. L. (1995). Optimal Aircraft Terrain-Following Analysis and Trajectory Generation. Journal of Guidance, Control, and Dynamics, 18(3), 555-560.

[7] Delahaye, D., Puechmorel, S., Tsiotras, P. & Feron, E. (2013). Mathematical models for aircraft trajectory design : A survey. 3rd ENRI International Workshop on ATM/CNS, 1-41

[8] Hong, K. W., Kim, S. J., Bang, H. C., Jeon, J. Y. & Choi, W.Y. (2023). Trajectory Generation Algorithm for Terrain Following based on Terrain Elevation. Journal of the Korean Society for Aeronautical & Space Sciences, 51(6), 391-398.

[9] Hahn, S., Lee, H., Lee, S., Choi, W. & Jung, J. (2023). A Study on the Terrain-Following Trajectory Generation Method Using Morphology and Circular Path. Journal of the Korean Society for Aeronautical & Space Sciences, 51(2), 93-102.

[10] Kang, S., & Yang, H. (2023). New Method for Generating Terrain Following Trajectory: NPR(Neighbor Point Re-positioning) Algorithm. Journal of the Korean Society for Aeronautical & Space Sciences, 51(9), 635-643.

[11] Lee, H., Hahn, S., Lee, S., Lee, S. & Seo, K. (2023). A Study on Terrain Profile Generation for Terrain Following. Journal of the Korean Society for Aeronautical & Space Sciences, 51(1), 49-56.

[12] Kang, S. H., Lee, H., Lee, S., Jeon, J. & Lim, D. (2023). A Study on Trajectory Generation for Terrain Following Using Brute Force Method and Circular Path Method. Journal of the Korean Society for Aeronautical & Space Sciences, 51(10), 685-692.